Determinants of the Detection Limit and Specificity of Surface-Based Biosensors

ARTICLE *in* ANALYTICAL CHEMISTRY · MAY 2013

Impact Factor: 5.64 · DOI: 10.1021/ac4012123 · Source: PubMed

6 AUTHORS, INCLUDING:

Berta Esteban Fernández de Ávila
University of California, San Diego
18 PUBLICATIONS **99** CITATIONS
SEE PROFILE

Herschel Max Watkins
Stanford University
13 PUBLICATIONS **61** CITATIONS
SEE PROFILE

José M Pingarrón
Complutense University of Madrid
333 PUBLICATIONS **6,493** CITATIONS
SEE PROFILE

analytical chemistry

Technical Note

pubs.acs.org/ac

Determinants of the Detection Limit and Specificity of Surface-Based Biosensors

Berta Esteban Fernández de Ávila,[†] Herschel M. Watkins,[‡] José M. Pingarrón,[†] Kevin W. Plaxco,[‡,§,⊥] Giuseppe Palleschi,[¶,∥] and Francesco Ricci*[,¶,∥]

[†]Departamento de Química Analítica, Facultad de CC. Químicas Universidad Complutense de Madrid, E-28040 Madrid, Spain

[‡]Department of Chemistry and Biochemistry, [§]Center for Bioengineering, and [⊥]Interdepartmental Program in Biomolecular Science and Engineering, University of California, Santa Barbara, California 93106, United States

[¶]Dipartimento di Scienze e Tecnologie Chimiche, University of Rome, Tor Vergata, Via della Ricerca Scientifica, 00133, Rome, Italy

[∥]Consorzio Interuniversitario Biostrutture e Biosistemi "INBB", Rome, Italy

Supporting Information

ABSTRACT: Here, we employ a model electrochemical DNA sensor to demonstrate that the detection limit and specificity of surface-based sensors often are not dependent on the true affinity of the probe for its target but are simply dependent on the effective probe concentration. Under these circumstances, the observed affinity (and thus the sensor's detection limit and specificity) will depend on the density with which the probes are packed on the surface of the sensor, the surface area, and even the volume of sample employed.

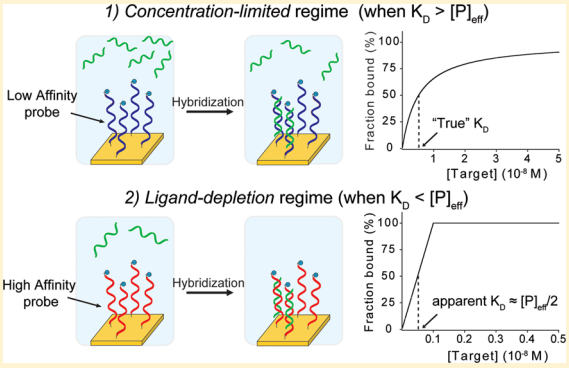

Due to their potential applications in, for example, point-of-care diagnostics, reagentless sensors that employ surface-bound biomolecules as their recognition elements have garnered significant recent attention.[1−4] Despite their increasingly widespread study, however, it appears that key aspects of the performance of these sensors are still widely misunderstood. Specifically, studies of the detection limits (the detection threshold) and specificity (the discrimination threshold) of sensors in this class often yield highly divergent answers. A clear example of this is provided by the voluminous literature on hybridization-based sensors for the detection of specific oligonucleotides sequences.[5] Although many authors have demonstrated robust discrimination between DNA sequences differing by as little as a single nucleotide, others have found that such surface-based sensors fail to achieve such high levels of specificity.[5−8] Equally alarmingly, other studies have reported detection limits differing by up to 3 orders of magnitude despite employing recognition elements expected to exhibit comparable dissociation constants.[5−8]

We believe that many of the above-described discrepancies arise due to the fact that surface-based biosensors can operate in either of two regimes, each of which produces different behavior. Specifically, the observed affinity (which, along with the sensor's gain and noise floor, defines its detection limit) of surface-based biosensors is ultimately defined by either the *concentration* or the *absolute number* of target molecules necessary to occupy a threshold fraction of the recognition probes on the sensor surface. Which of these two regimes a sensor is operating in, however, depends on the specifics of the true affinity of the probe, the density with which it is packed onto the sensor's surface, and even the sample volume under interrogation.

In a regime in which the number of target molecules participating in probe/target complexes is low relative to the total number of target molecules in the sample, occupancy is defined by the concentration of the target relative to the affinity (K_D) with which it binds the probe (Figure 1, top). Under these *concentration-limited* conditions, binding is generally well described using a simplified hyperbolic Langmuir isotherm[9] with a midpoint value reflecting dissociation constant (K_D) of the probe/target complex:

$$S([T]) = S_0 + (S_B - S_0)\frac{[T]}{[T] + K_D} \quad (1)$$

where $S([T])$ is the measured output signal at target concentration $[T]$, S_0 is the background signal observed in the absence of target, and S_B is the signal observed at saturating target concentrations. These *concentration-limited* conditions are typically met (and eq 1 obeyed) when the sample volume is

Received: April 25, 2013
Accepted: May 29, 2013
Published: May 29, 2013

   dx.doi.org/10.1021/ac4012123 | *Anal. Chem.* 2013, 85, 6593−6597

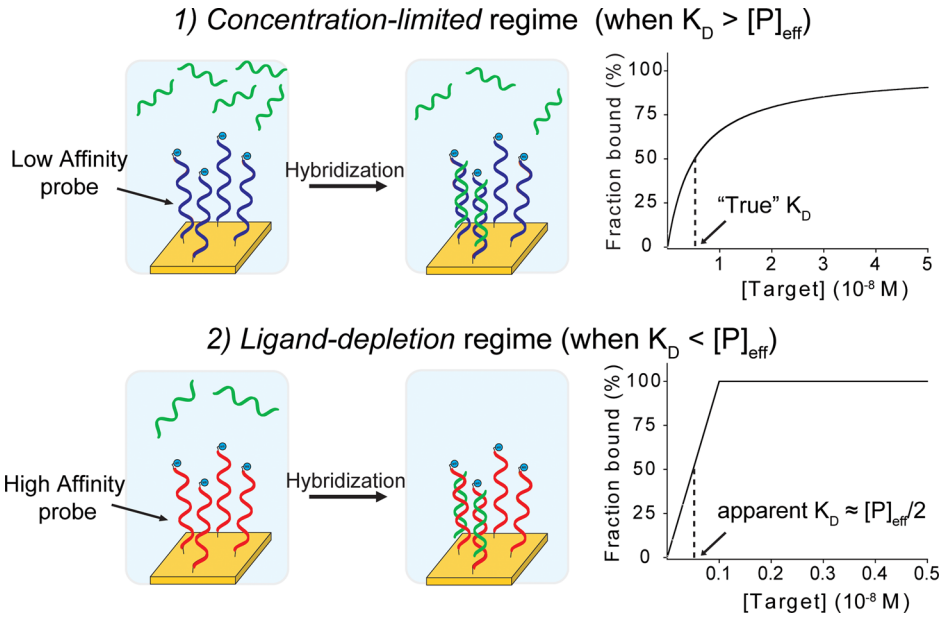

Figure 1. Surface-based sensors can operate in two regimes. (Top) The first, the *concentration-limited* regime, occurs when the effective probe concentration, $[P]_{eff}$ (i.e., the concentration that would be seen if the probe were released from the surface and dispersed through the sample volume), is lower than the true affinity of the probe for its target (K_D). Under these conditions, occupancy is defined by the molar concentration of the target (relative to K_D) and a classic Langmuir-isotherm is observed for which the midpoint reflects the true K_D of the probe/target complex. (Bottom) Conversely, if the true affinity of the probe for its target is very high (i.e., the true K_D is low and is lower than the effective probe concentration), significant occupancy is observed even at very low target concentrations, concentrations low enough that the number of target molecules bound to the probe can be of similar magnitude to the total number in the sample. Under these *ligand-depletion* conditions, occupancy is no longer defined by the true affinity of the probe or the concentration of the target in solution but instead by the total number of ligand (target) molecules in the sample relative to the total number of probes on the sensor surface. In this latter case, a bilinear binding curve is observed with a midpoint at a target concentration half of the effective probe concentration ($[P]_{eff}/2$). In this work, we perform an exhaustive, quantitative study of the key determinants (e.g., surface probe density, sample volume, and true K_D) that define these two regimes, using as our test-bed an electrochemical DNA sensor.[2]

high (and thus the ratio of target molecules to probe molecules is high) and the affinity of the probe for its target is poor (thus requiring relatively high target concentrations in order to achieve detectable occupancy).

In contrast to the *concentration-limited* regime, quite different behavior occurs under conditions in which probe occupancy is limited instead by the absolute number of target molecules in the sample. Specifically, if the probe binds its target very avidly (i.e., K_D is very low), each additional molecule of target in a sample will bind to a probe until all of the probes are saturated (Figure 1, bottom). Under these conditions, the relationship between occupancy and target concentration is bilinear,[10−13]

$$S([T]) = S_0 + (S_B - S_0)\frac{[T]}{[P]_{eff}} \quad (2)$$

where $[P]_{eff}$, the effective probe concentration, is the concentration of probe were it liberated from the surface and dispersed throughout the sample volume. Under these *ligand-depletion* conditions, occupancy is no longer defined by the true affinity of the probe or the concentration of the target in solution but instead by the total number of target molecules in solution (which depends, in turn, on both the sample volume and the target concentration) relative to the number of probe molecules (which is dependent on probe packing density and the surface area of the sensor). When this occurs, the midpoint of a concentration/output plot (the "apparent" affinity, K_{D_app}) does not reflect the true affinity of the probe for its target (K_D) but is instead given by $[P]_{eff}/2$.

There thus exist two regimes. If the probe's K_D is greater than $[P]_{eff}$, the sensor is in the *concentration-limited* regime, and the observed K_D reflects the true affinity of the probe for its target (Figure 1, top). If, in contrast, the probe's K_D is less than $[P]_{eff}$, the sensor is in the *ligand-depletion* regime and the observed K_D does not reflect the "true" K_D. Under this condition, the observed K_D will instead depend on the experimental conditions including probe density, surface area, and sample volume (Figure 1, bottom). In principle, the shape of a binding curve should discriminate between the *concentration-limited* regime (when the midpoint reflects the true affinity) and the *ligand-depletion* regime (where it does not). In practice, however, discriminating between a bilinear curve and a hyperbolic curve can prove difficult (Figure 2), leading to the discrepancies discussed above regarding the observed affinities and specificities of surface-based sensors. Here, we explore this important issue quantitatively, demonstrating the ease with which the two regimes can be confused and describing several quantitative tests to distinguish between them.

MATERIALS AND METHODS

A 27-base 5′ thiol-, 3′ methylene blue (MB)-modified probe DNA was obtained from Biosearch and employed as the signaling probe DNA. Target DNA sequences (perfect match and 1-base mismatch) were obtained from Sigma-Aldrich (see Supporting Information for sequences). E-DNA sensors were fabricated on gold screen printed-electrodes[14] as previously described[2] (see Supporting Information for details). We note

dx.doi.org/10.1021/ac4012123 | Anal. Chem. 2013, 85, 6593−6597

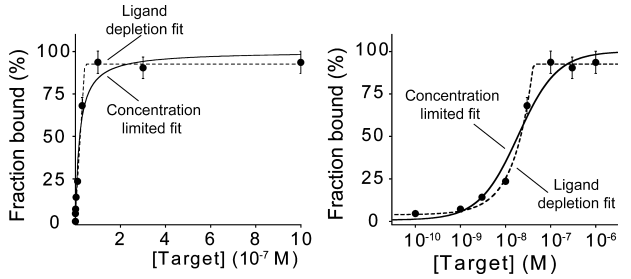

Figure 2. In practice, differentiating between the *concentration-limited* and *ligand-depletion* regimes with simple binding curve experiments is often quite difficult, leading to significant discrepancies in the interpretation of results derived using surface-based sensors. Here, we expand on this theme by exploring the key determinants of the switch between these two regimes and demonstrating several tests that help discriminate between them. Shown are actual experimental data obtained using the E-DNA electrochemical biosensor[2] described below and fit with both *ligand-depletion* and *concentration-limited* equations using a linear (left) and the more commonly used logarithmic (right) scale. For a matter of clarity in these binding curves and in those in the following figures, error bars have been depicted for only some points on each curve and represent the average and standard deviations of measurements performed on at least three independent sensors.

that the use of gold screen printed-electrodes with E-DNA sensors was recently described achieving similar results than those obtained with classic rod gold electrodes.[2b] All experiments were performed in 150 mM NaCl/50 mM potassium phosphate buffer, pH 7.0. Binding curves were obtained by interrogating with square wave voltammetry (see Supporting Information for details) each sensor in buffer solution (background signal) and at different target concentrations until signal suppression was stable. The signal changes have been normalized on a 0−100 scale to allow for more ready interpretation of the results. Probe surface-density was determined using a previously established method[15] based on the use of RuHex (see Supporting Information for details).

RESULTS AND DISCUSSION

As a test bed to explore the *concentration-limited* and *ligand-depletion* regimes, we have employed an electrochemical-DNA (E-DNA) sensor as our model system.[2] Specifically, we have employed an E-DNA sensor composed of a 27-base linear DNA probe covalently modified on the 3′ terminus with a redox reporter (methylene blue, MB) and on the 5′ terminus with a long-chain alkane thiol, which enables chemi-absorption to the gold electrode surface via a gold−thiol bond. In the absence of a complementary target, the probe's structure allows the redox reporter to move into proximity with the electrode, supporting efficient electron transfer.[2] Upon hybridization to its target, the linear probe assumes a relatively rigid, double-stranded conformation that reduces the efficiency with which the reporter approaches the surface, reducing electron transfer rates, and decreasing the Faradic current observed when the sensor is interrogated using square wave voltammetry.[2]

The true affinity of our linear DNA probes is very high: the K_D for a fully complementary 27-base target−probe duplex is estimated to be subfemtomolar (calculated using the *m-fold* algorithm[16]). Our model sensor thus operates under *ligand-depletion* conditions for any reasonable set of sample volume, probe density, and sensor surface area values. The experimental results obtained by challenging the sensor with increasing concentrations of its target nevertheless fit both the bilinear and Langmuir-isotherm curves with effectively identical precision (Figure 2), highlighting the sometimes difficult nature of distinguishing between the two types of behavior.

To demonstrate how working under *ligand-depletion* regime can lead to misinterpretation of observed affinity, we have fabricated a set of matching E-DNA sensors varying only in probe density and, thus, when deployed against a fixed sample volume, varying in effective probe concentration. Challenging these with the same 27-base, perfectly matched target produces binding curves with midpoint values ranging from 3.1 ± 0.1 nM at the lowest probe density to 16.3 ± 0.2 nM at the highest (Figure 3, left). This probe-density dependence, which occurs

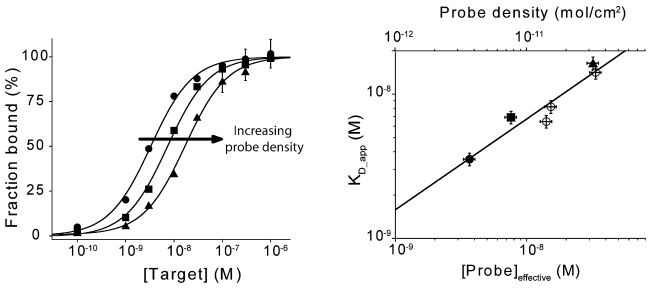

Figure 3. In the *ligand-depletion* regime, the apparent affinity of a sensor varies with increasing probe density. (left) Shown are binding curves obtained from sensors differing in probe density (left to the right: 0.37, 0.76, and 3.2 × 10^{-11} mol/cm^2). With a surface area of 0.07 cm^2 and in a sample volume of 70 μL, these values correspond to effective probe concentrations of 3.7 to 32.6 × 10^{-9} M. (right) Under these (fixed sample volume) experimental conditions, the apparent affinities of the sensors are well correlated with their probe densities.

despite the fact that, to a first approximation, the true affinity of the probe for its target should be independent of probe density, is a clear signal of the *ligand-depletion* regime. That is, here the true affinity of the probe for its target is much lower than the effective concentration of probe molecules in the sample, and thus, every target molecule in the sample binds to a probe until the limit in which all probes are bound. Given this, the increase in effective probe concentration associated with increasing probe-density leads, in turn, to an increase in the apparent affinity. Consistent with this, K_{D_app} is proportional to probe density under this set of experimental conditions (i.e., fixed sample volume) (Figure 3, right).

The effective probe concentration and, thus, the apparent affinity observed in the *ligand-depletion* regime also depends on sample volume.[11] To demonstrate this, we have challenged identical sensors (i.e., all of the same probe density and surface area) against a range of sample volumes (Figure 4). As expected, the K_{D_app} observed for the smallest sample volume is about 2 orders of magnitude higher than that of the largest.

An important consideration is that, as long as we remain in the *ligand-depletion* regime, the apparent affinity is independent of the true affinity. To demonstrate this, we have measured the apparent affinity of a sensor against a set of targets differing in true affinity. We did so by using perfectly matched targets of different length ranging from 27 (higher true affinity) to 13-bases (lower true affinity). Of note, all these targets have estimated subnanomolar true affinities. While there was a clear trend in total signal suppression (Figure 5, left), with longer targets creating greater signal changes (due to the increased rigidity of the longer double-stranded probe−target duplexes[2b,c]), the apparent affinity (3.6 ± 0.3 nM) is, to within

dx.doi.org/10.1021/ac4012123 | Anal. Chem. 2013, 85, 6593−6597

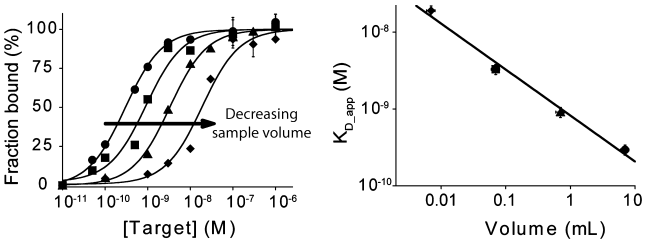

Figure 4. Under *ligand-depletion* regime, apparent affinity depends strongly on sample volume because this changes the effective probe concentration in solution. Here, we used a 27-base target with an estimated femtomolar true affinity that assures the sensor is under *ligand-depletion* regime at all the volumes tested. Accordingly, upon decreasing the sample volume (thus increasing the effective probe concentration), we observe a consistent increase in the observed K_{D_app} of the sensor.

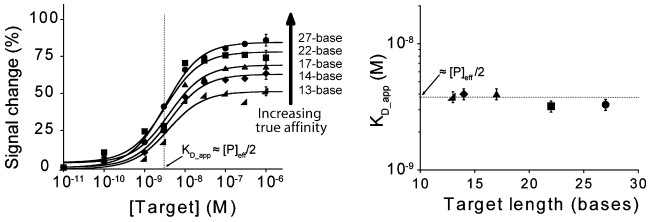

Figure 5. Under *ligand-depletion* regime, the apparent affinity is independent of the true affinity. To demonstrate this, we have challenged identical sensors with targets varying in length and thus of varying true affinity. Of note, the true affinities of all these different targets are all in the subnanomolar range, and thus, they all operate under *ligand-depletion* regime in this experimental condition. While longer targets produce greater ultimate signal change (due to their larger effects on probe dynamics[2b,c]) (left), the apparent affinity remains constant (right).

experimental error, independent of target length (Figure 5, right). Again, this is because the apparent affinity observed in this regime is defined by the effective probe concentration, which does not vary with target length or affinity.

The inability to differentiate between targets differing in true affinity suggests a reason for the often poor specificity reported for surface-based biosensors. If the true affinity for both a perfectly matched and single-base mismatched target are *both* below the minimum apparent affinity that can be measured, then both targets will produce *the same apparent affinity*. To demonstrate this, we have measured the apparent affinity of our sensor for mismatched targets of various lengths and compared these values to the affinities measured for the perfectly matched target of the same length. For example, using long (i.e., high true affinity), 27-base targets, the apparent affinity for the perfectly matched target, 2.7 ± 0.3 nM, is nearly indistinguishable from the 3.4 ± 0.2 nM observed for the mismatched target (Figure 6, left). Indeed, despite their poorer true affinity, this difficulty holds even for much shorter targets (e.g., 17-base target; Figure 6, center). Only for the very shortest targets (13-base) do we observe a clear difference between perfectly matched (K_{D_app} = 3.8 ± 0.4 nM) and single-base mismatched (71.2 ± 0.6 nM) targets; only when the true affinity of the mismatched target becomes extremely poor do we break out of the *ligand depletion* regime (Figure 6, right). The *ligand-depletion* regime should thus be avoided if optimal discrimination efficiency is required.

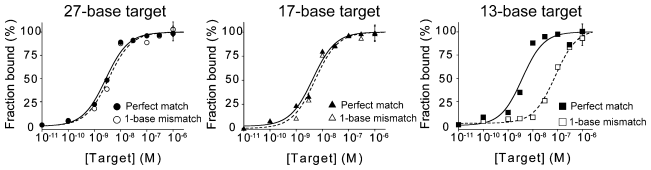

Figure 6. Good discrimination efficiency is only observed when we break out of the *ligand-depletion* regime (i.e., when the true K_D for the mismatch is greater than the effective probe concentration). Shown are binding curves for perfectly matched and 1-base mismatched targets of different lengths. While the apparent affinity for the three perfectly matched targets is the same (all are in the *ligand-depletion* regime), we only observe significant discrimination with the shortest mismatched target (right), the affinity for which is poor enough that is in the *concentration-limited* regime.

CONCLUSIONS

Here, we have shown that the observed affinity of reagentless surface-based biosensors is often defined, not by the true affinity of its probe, but instead by the effective probe concentration. Under these circumstances, the observed affinity (and thus the sensor's detection limit and specificity) will depend on the density with which the probes are packed on the surface of the sensor, the surface area, and even the volume of sample employed. Under this *ligand-depletion* regime, the minimum observable affinity (and so the detection limit) thus depends on the experimental setup more than on the actual true affinity of the probe itself. Any attempt to improve detection limits without changing the experimental conditions faces significant inherent challenges. Being in the *ligand-depletion* regime also diminishes a sensor's specificity. Indeed, optimal specificity is only achieved in the *concentration-limited* regime, and thus, to achieve good specificity, experimental conditions must be tuned to push the sensor into this regime. Failure to do this may account for some previously unexplained discrepancies in the ability of surface-based DNA biosensors to discriminate between perfectly matched and mismatched targets.[5−8] More generally, we advise our readers to pay careful attention to the conditions under which the binding curves of surface-based biosensors are derived, particularly when working with high affinity recognition elements.

ASSOCIATED CONTENT

Supporting Information

Additional information as noted in the text. This material is available free of charge via the Internet at http://pubs.acs.org

AUTHOR INFORMATION

Corresponding Author

*E-mail: francesco.ricci@uniroma2.it.

Notes

The authors declare no competing financial interest.

ACKNOWLEDGMENTS

This work was supported by the Italian Ministry of University and Research (MIUR) through the project FIRB "Futuro in Ricerca" the Marie Curie International Outgoing Fellowship within the seventh European Community Framework Programme (PIOFGA-2011-298491 to F.R.). B.E.F.A. has a FPI fellowship from the Spanish Ministerio de Ciencia e Innovación, and H.M.W. is a Whitaker Fellow.

REFERENCES

(1) (a) Cui, Y.; Wei, Q.; Park, H.; Lieber, C. M. *Science* **2001**, *293*, 1289. (b) Janshoff, A.; Galla, H.; Steinem, C. *Angew. Chem., Int. Ed.* **2000**, *39*, 4004. (c) Homola, J. *Anal. Bioanal. Chem.* **2003**, *377*, 528. (d) Wang, J. *Biosens. Bioelectron.* **2006**, *21*, 1887.

(2) (a) Lubin, A. A.; Plaxco, K. W. *Acc. Chem. Res.* **2010**, *43*, 496. (b) Kang, D.; Vallee-Belisle, A.; Porchetta, A.; Plaxco, K. W.; Ricci, F. *Angew. Chem., Int. Ed.* **2012**, *51*, 6717. (c) Ricci, F.; Lai, R. Y.; Plaxco, K. W. *Chem. Commun.* **2007**, *36*, 3768.

(3) (a) Vollmer, F.; Arnold, S. *Nat. Methods* **2008**, *5*, 591. (b) Maehashi, K.; Katsura, T.; Kerman, K.; Takamura, Y.; Matsumoto, K.; Tamiya, E. *Anal. Chem.* **2007**, *79*, 782. (c) Gooding, J. J. *Electroanalysis* **2002**, *14*, 1149. (d) Daniels, J. S.; Pourmand, N. *Electroanalysis* **2007**, *19*, 1239.

(4) Rant, U.; Arinaga, K.; Scherer, S.; Pringsheim, E.; Fujita, S.; Yokoyama, N.; Tornow, M.; Abstreiter, G. *Proc. Natl. Acad. Sci. U.S.A.* **2007**, *104*, 17364.

(5) (a) Paleček, E.; Bartošík, M. *Chem. Rev.* **2012**, *112*, 3427. (b) Wang, J. *Anal. Chim. Acta* **2001**, *469*, 63. (c) Drummond, T. G.; Hill, M. G.; Barton, J. K. *Nat. Biotechnol.* **2003**, *21*, 1192.

(6) (a) Fritz, J.; Cooper, E. B.; Gaudet, S.; Sorger, P. K.; Manalis, S. R. *Proc. Natl. Acad. Sci. U.S.A.* **2002**, *99*, 14142. (b) Taton, T. A.; Mirkin, C. A.; Letsinger, R. L. *Science* **2000**, *289*, 1757. (c) Nelson, B. P.; Grimsrud, T. E.; Liles, M. R.; Goodman, R. M.; Corn, R. M. *Anal. Chem.* **2001**, *73*, 1.

(7) (a) Peterson, A. W.; Heaton, R. J.; Georgiadis, R. *J. Am. Chem. Soc.* **2000**, *122*, 7837. (b) Peterson, A. W.; Wolf, L. K.; Georgiadis, R. M. *J. Am. Chem. Soc.* **2002**, *124*, 14601. (c) Maruyama, Y.; Terao, S.; Sawada, K. *Biosens. Bioelectron.* **2009**, *24*, 3108. (d) Zhang, J.; Chen, J. H.; Chen, R. C.; Chen, G. N.; Fu, F. F. *Biosens. Bioelectron.* **2009**, *25*, 815.

(8) (a) Gasparac, R.; Taft, B. T.; Lapicrre-Devlin, M. A.; Lazareck, A. D.; Xu, J. M.; Kelley, S. O. *J. Am. Chem. Soc.* **2004**, *126*, 12270. (b) Kafka, J.; Pänke, O.; Abendroth, B.; Lisdat, F. *Electrochim. Acta* **2008**, *53*, 7467. (c) Yang, W.; Lai, R. Y. *Electrochem. Commun.* **2011**, *13*, 989.

(9) Van De Weert, M.; Stella, L. *J. Mol. Struct.* **2011**, *998*, 145.

(10) Hulme, E. C.; Trevethick, M. A. *Br. J. Pharmacol.* **2010**, *161*, 1219.

(11) Carter, C. M. S.; Leighton-Davies, J. R.; Charlton, S. J. *J. Biomol. Screening* **2007**, *12*, 255.

(12) Goldstein, A.; Barrett, R. W. *Mol. Pharmacol.* **1987**, *31*, 603.

(13) Wells, J. W.; Birdsall, N. J.; Burgen, A. S.; Hulme, E. C. *Biochim. Biophys. Acta* **1980**, *632*, 464.

(14) Ricci, F.; Amine, A.; Moscone, D.; Palleschi, G. *Biosens. Bioelectron.* **2007**, *22*, 854.

(15) (a) Steel, A. B.; Herne, T. M.; Tarlov, M. J. *Anal. Chem.* **1998**, *70*, 4670. (b) Lao, R.; Song, S.; Wu, H.; Wang, L.; Zhang, Z.; He, L.; Fan, C. *Anal. Chem.* **2005**, *77*, 6475.

(16) Markham, N. R.; Zuker, M. *Nucleic Acids Res.* **2005**, *33*, 577.

dx.doi.org/10.1021/ac4012123 | *Anal. Chem.* 2013, 85, 6593−6597